

Particle Swarm Optimization of Fuzzy Fractional PD^μ+I Controller of a PMDC Motor for Reliable Operation of Wire-Feeder Units of GMAW Welding Machine

Abstract. In this article, we consider the development of an optimal control approach based on fuzzy fractional PD^μ+I controller to improve the speed error-tracking and control capability of a permanent magnet DC Motor (PMDC) driven wire-feeder systems (WFSs) of gas metal arc welding (GMAW) process. The proposed controller employs an optimized fractional-order proportional derivative + integral (PD^μ+I) controller that serves to eliminate oscillations, overshoots, undershoots and steady state fluctuations of the PMDC motor and makes the wire-feeder unit (WFU) has fast and stable starting process as well as excellent dynamic characteristics. The fixed controller parameters are meta-heuristically selected via a particle swarm optimization (PSO) algorithm. Numerical simulations are performed in MATLAB/SIMULINK environment and the performance of the proposed fuzzy fractional PD^μ+I controller is validated. The simulation tests clearly demonstrate the significant improvement rendered by the proposed fuzzy PD^μ+I controller in the wire-feeder system's reference tracking performance, torque disturbance rejection capability and robustness against model uncertainties.

Streszczenie. Analizowano optymalne sterowanie silnikiem zDC z magnesami trwałymi wykorzystujące sterownik fuzzy PD^μ+I. Silnik stosowany jest do sterowania procesem spawania. Układ sterowania wykorzystuje sterownik proporcjonalny ułamkowego rzędu i całkujący zapewniający dobrą dynamikę układu – bez oscylacji (Wykorzystanie algorytmu optymalizacji rojowej o sterownika fuzzy do sterowania silnikiem prądu stałego z magnesami trwałymi wykorzystywanym w procesie spawania).

Keywords: GMAW process, wire-feeder system (WFS), fuzzy fractional PD^μ+I controller, particle swarm optimization (PSO) algorithm.

Słowa kluczowe: silnik prądu stałego z magnesami, optymalizacja rojowa, logika rozmyta, spawanie

Introduction

Nowadays, joining metals is a fundamental aspect of modern industrialized operations such as the ship building, automotive, and construction industries. It can be accomplished by different arc welding techniques. Among the various types of welding the typical GMAW process is the most frequently employed and economically important welding process for joining metals. It is preferred for its flexibility, rapidity and can be utilized for both manual and automatic modes of welding for wide range of ferrous and non-ferrous metal pieces [1].

Consistency and high quality welding procedures are the key issues to maintain and increase the overall product quality. During GMAW process, the electrode wire is melted and liquid droplets are formed at the tip of the electrode. When detaching from the electrode, the droplets transfer both mass and heat into the weld pool. In order to achieve quality welds, the transfer process must be controlled. One of the strategies to control the quality of the weld is to maintain the set values of welding current and arc length to achieve the preferred values of heat and mass transfer to the work-piece. The control variables selected are, the wire feed rate and the open circuit voltage, which are utilized to control the current and arc length of the GMAW process [2].

Large swing in wire feed rate results in large increased stress in PMDC motor and in welding current during welding process. This changes in wire feed rate causes the arc breaking, affecting the arc stability which ceases the welding operation. Therefore, wire-feeder system (WFS) is an important subsystem of typical automatic GMAW process. It should not only prevent the fracture and vibration of wire from occurring, but also guarantee the high speed of wire feed to meet the need of high rate of automatic welding production. Therefore, the control of wire feed rate for the WFS is the key technologies of the wire-feeder units (WFUs), which has a strong impact on the welding quality.

The available WFUs are designed for constant wire feed rate and feature a large inertia and static friction due to the reduction gearbox and the eccentricities in the wire roller mechanism, and also due to the wire spool and the

important frictions of the wire feed path [3]. Thus, this mechanical dynamic is very slow as compared to the arc welding melting process [4]. Many solutions have been introduced in the literature to improve the wire feed speed responses of the WFUs either by developing new mechanisms with various types of permanent magnet DC (PMDC) motors or by designing robust wire feeder controllers [4-8].

The accurate design of wire-feeder controller is essential to provide productivity, wide range welding capability, and comfort level to the welder user. One of the most widely used wire-feed speed regulation schemes is the proportional-integral-derivative (PID) controller [9]. It is a simple and stable controller that provides a reliable control effort. However, the design of the accurate wire-feeder controller for PMDC motor of the WFUs using the traditional PID controller require accurate modeling of the PMDC motor that considers the non-linear dynamics.

It is possible to use a traditional PID regulator to control the wire feed speed of the WFUs [9]. However, traditional PID controllers do not yield reasonable performance over a wide range of working conditions.

Variable structure sliding mode controllers (SMCs) offer a robust control effort [10-12]. However, they inject chattering in the response and expend a lot of control energy.

The augmentation of integer-order PID controllers with fractional calculus enables the control strategy to compensate for the effects of the un-modeled intrinsic nonlinearities associated with real-world dynamical systems [13]. The fractional-order PID controller (PI^λD^μ controller) comprises two extra degrees of freedom an integrator of order $\lambda \in \mathbb{R}^+$ and a differentiator of order $\mu \in \mathbb{R}^+$ [14]. The addition of a fractional-order parameter, along with the three PID controller gains, increases the degree of freedom and design flexibility of the controller [15]. On the other hand, the advantages of fractional PI^λD^μ controller and artificial intelligence can be incorporated to improve the setting efficiency and system performances [16].

The fuzzy logic controller (FLC) presents a methodical procedure to design controllers for much class of systems through the employ of heuristic information. Fractional hybrid fuzzy logic controllers are the results of the mixture of FLCs and fractional $PI^{\lambda}D^{\mu}$ controller. Under such combination, the FLC based on fractional $PI^{\lambda}D^{\mu}$ controller has a better performance and robustness than conventional fractional $PI^{\lambda}D^{\mu}$ for a wide range of dynamical systems [16]. The present study investigates the effectiveness of tuned fuzzy fractional $PD^{\mu}+I$ controller at producing better performance compared to traditional PID controller, fractional-order PID (FOPID) controller, and even fuzzy fractional-order PID (FFOPID) controller. Parameter adjustment is a vital step to develop applications with fuzzy fractional $PD^{\mu}+I$ controller.

This procedure is long and time consuming, since it is commonly conducted through trial and error. Therefore, the parameter calibration in fuzzy fractional $PD^{\mu}+I$ controllers can be handled by evolutionary optimization methods. Due to its faster convergence and flexibility, a particle swarm optimization (PSO) algorithm is adopted in this article for the optimal adjustment of the proposed fuzzy fractional $PD^{\mu}+I$ controller.

Based on previous consideration and analysis, the first major contribution of this article is the methodic design and optimal time domain tuning of a robust fuzzy fractional $PD^{\mu}+I$ controller. The second contribution has been the implementation of tuned fuzzy fractional $PD^{\mu}+I$ controller in first time for speed tracking task of PMDC motor driven WFSs of GMAW process. The performance of the considered fuzzy fractional $PD^{\mu}+I$ is compared with other three potential controllers namely FOPID, FFOPID and conventional PID controller for the speed tracking task. Moreover, the robustness testing against model uncertainties and external disturbance is also carried out to witness the effectiveness of the proposed fuzzy fractional $PD^{\mu}+I$ controller.

Dynamics of GMAW Process

In the GMAW process, the welding inverter controls the open circuit voltage $V_{oc}(V)$ between the contact tip tube and the work-piece. In addition, the wire feed servo motor rotates a set of pinch rollers, which forces the wire into the torch head and through the contact tube whereupon the wire is consumed by the GMAW process as illustrated in Figure 1.

The wire feed servo motor is in itself a feedback controlled system which is capable of delivering wire to the weld process at a controlled wire feed rate; increasing or decreasing the wire feed speed $V_f(m/s)$ on the wire feeder servo motor increases or decreases the welding current $I_w(A)$ as well as the metal transfer mode [5].

In majority of cases, the value of $V_f(m/s)$ is taken constant at desired value. For the purposes of this derivation, the wire feed rate is considered to be the input. The arc dynamics form the plant $I_a(m)$ and the welding current $I_w(A)$ is taken to be the output.

The dynamic equation for the electrical circuit of the GMAW process, is

$$(1) \quad V_{oc} = L_1 \frac{dI_w}{dt} + R_s I_w + V_{arc}$$

where: $V_{oc}(V)$ represents the open circuit voltage of arc welder power supply, $I_w(A)$ is the instantaneous welding current, $R_s(\Omega)$ is the Thevenin resistance of arc welder power supply plus cabling resistance and $L_1(mH)$ is the inductance of arc welder power supply.

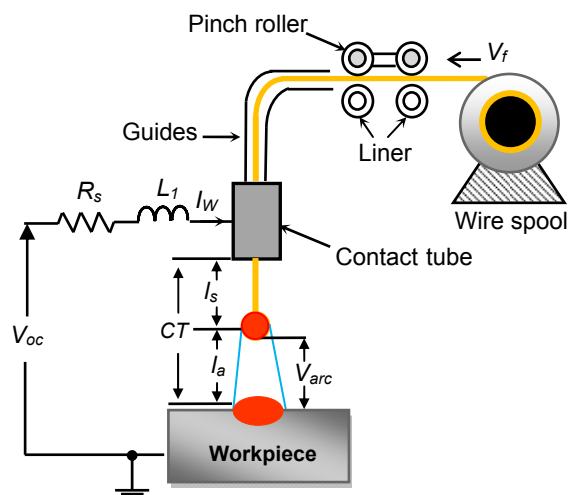


Fig.1. Physical representation of WFS for GMAW process

The dynamic equation of arc voltage $V_{arc}(V)$ is expressed as [4].

$$(2) \quad V_{arc} = k_a I_a + k_p I_w + V_c$$

where: k_a , k_p , V_c are parameters of arc characteristics, and $I_a(m)$ is the arc length.

The dynamic equation of arc length $I_a(m)$, is

$$(3) \quad \frac{dI_a}{dt} = V_m - V_f$$

where: $V_m(m/s)$ represents the wire melting rate may be expressed as

$$(4) \quad V_m = k_m I_w$$

where: k_m is the coefficient of wire melting rate.

The dynamic equation of the power source V_{oc} , is

$$(5) \quad V_{oc} = (R_u + k_1 I_w) k_0$$

where: $R_u(V)$ is the control input of the power source, k_0 is gain of power source and k_1 is feedback gain.

Mathematical Model of PMDC Motor Driven Wire-Feeder System (WFS)

The graphic illustration of power circuit of the wire-feed servo motor control is depicted in Figure 2.

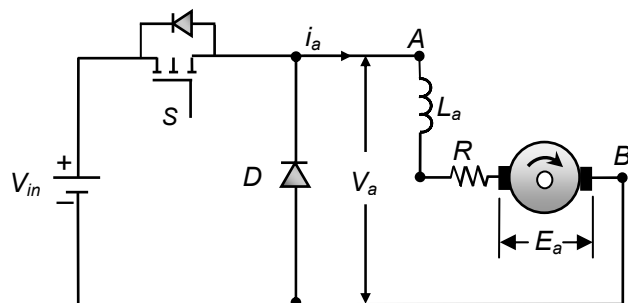


Fig.2. Power circuit for the wire-feed servo motor control

where: the PMDC motor control variables are DC input voltage $V_a(V)$ and load torque $T_L(N.m)$. In WFUs, T_L depends on diameter $d(cm)$ of electrode wire and its material composition. For a particular application it could be considered as constant.

The PMDC motor output variables are the wire feed speed $V_f(m/s)$, the angular displacement of the motor shaft $\theta(rad)$ and the armature current $i_a(A)$.

The PMDC motor's dynamic equations can be developed based on the Kirchhoff's voltage law around the armature circuit and the Newton's moment law using the following formulas.

$$(6) \quad V_a = L_a \frac{di_a}{dt} + R_a i_a + k_2 \frac{d\theta}{dt}$$

$$(7) \quad J \frac{d^2\theta}{dt^2} + f \frac{d\theta}{dt} = k_3 i_a$$

$$(8) \quad V_f = k_4 \frac{d\theta}{dt}$$

where: $V_a(V)$ is the armature voltage, $i_a(A)$ is the armature current, $R_a(\Omega)$ is the armature resistance, $L_a(mH)$ is the armature inductance, $\theta(rad)$ is the angular displacement of the motor shaft, $V_f(m/s)$ is the wire feed rate, $J(kg \cdot m^2)$ is the moment of inertia of the motor and mechanical load converted to the motor shaft, $f(Nm \cdot s)$ is the coefficient of viscosity of the motor and mechanical load converted to the motor shaft, k_2 , k_3 and k_4 are constants.

Taking the Laplace transform of the expressions (6–8), the configuration of the control unit of the PMDC motor can be shown as the block diagram in Figure 3.

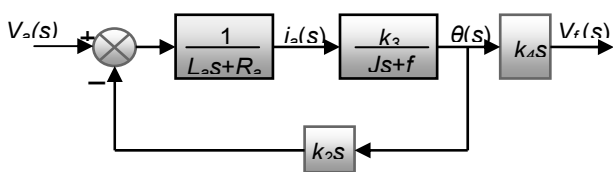


Fig.3. Block diagram of wire-feed motor

According to Figure 3, the transfer function can be derived as

$$(9) \quad \frac{\theta(s)}{V_a(s)} = \frac{k_3}{s(L_a J s^2 + (L_a f + R_a J)s + R_a f + k_3 k_2)}$$

If the motor inductance, L_a , is neglected, then

$$(10) \quad \frac{\theta(s)}{V_a(s)} = \frac{k_3}{s(R_a J s + R_a f + k_3 k_2)} = \frac{k_m}{s(T_m s + 1)}$$

The gain of the wire-feed mechanism is written by (11)

$$(11) \quad k_m = \frac{k_3}{R_a f + k_3 k_2}$$

The time constant of the wire-feed mechanism is

$$(12) \quad T_m = \frac{R_a J}{R_a f + k_3 k_2}$$

Therefore, the transfer function of the wire-feed mechanism may be simplified as follow.

$$(13) \quad \frac{V_f(s)}{V_a(s)} = \frac{K_m k_4}{T_m s + 1}$$

The control-block diagram of the regulated wire-feed rate system may be simplified as shown in Figure 4, $R_v(s)$

represents the control input to the wire-feed motor and k_5 is the open-loop gain of the motor circuit [4]. According to Figure 4, the transfer function of the system and its dynamic characteristics can be derived as

$$(14) \quad \frac{L_a(s)}{R_v(s)} = \frac{k_5 K_m k_4}{T_m s^2 + s + k_5 K_m k_4 k_a}$$

$$(15) \quad \zeta = \frac{1}{2\sqrt{T_m k_5 K_m k_4 k_a}}$$

$$(16) \quad \omega_n = \sqrt{\frac{k_5 K_m k_4 k_a}{T_m}}$$

$$(17) \quad \omega_d = \sqrt{\frac{4T_m k_5 K_m k_4 k_a - 1}{2T_m}} \approx \frac{\sqrt{k_5 K_m k_4 k_a}}{T_m}$$

$$(18) \quad \sigma = \zeta \omega_n = \frac{1}{2T_m}$$

In the most instances, $T_m k_5 K_m k_4 k_a > 1$ and $0 < \zeta < 1$; therefore the system is in an under-damped state.

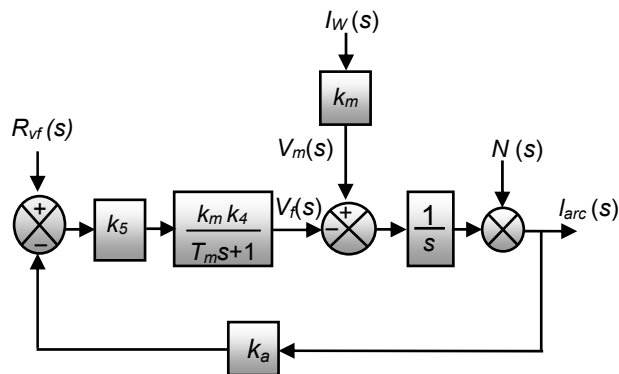


Fig.4. Block diagram of regulated wire feed-rate system

Table 1 presents parameters and their values used in simulation model of wire-feed motor control :

Table 1. Parameters for wire-feed motor

Parameters of PMDC motor	Symbol	Parameter value
Armature resistance	R_a	1.2 Ω
Armature inductance L_a	L_a	0.96 mH
Rotary inertia	J	$1 \cdot 10^{-7}$ kg.m ²
Viscous damping coefficient	f	$1.29 \cdot 10^{-3}$ N.m.s/rad
Back EMF constant	k_2	0.0573 V.s/rad
Electromagnetic torque constant	k_3	0.0573 N.m/A

Mathematical Model of PMDC Motor Driven Wire-Feeder System (WFS)

Generally, the wire feed speed controller is designed to realize accurate and robust optimal tracking of the preferred wire speed from no load to full load conditions. Hence, in this article a robust fuzzy fractional PD ^{λ} +I controller is used to optimally reach the design objectives.

A. Fractional order PID controller

The fractional PID (FOPID) controller is proposed by Podlubny which named it PI ^{λ} D ^{μ} controller. It has λ and μ as fractional components of integrator and differentiator respectively. The PI ^{λ} D ^{μ} controller, in the time-domain, is given by the expression (19)

$$(19) \quad u_{FOPID}(t) = k_p e(t) + k_i D_i^{-\lambda} e(t) + k_d D_i^{\mu} e(t)$$

The generalized transfer function of the PI^λD^μ controller is given as follows

$$(20) \quad G_{FOPID}(s) = k_p + k_i s^{-\lambda} + k_d s^{\mu}, (\lambda, \mu > 0)$$

where k_p , k_i and k_d are proportional, integral and derivative gains constants, respectively, λ and μ are fractional order of the integral and derivative term.

The term s^{λ} in expression (20) has a fractional order that makes it difficult to implement [16], [17]. Hence, in this article, the fractional integral operator is approximated using a 5th order Oustaloup's recursive filter for the practical implementation of a FOPID controller in a digital computer. The Oustaloup's approximation of s^{λ} is given by (21)

$$(21) \quad s^{\beta} = \prod_{n=1}^N \frac{1 + \frac{s}{\omega_{z,n}}}{1 + \frac{s}{\omega_{p,n}}}$$

where N is the order of approximation. The aforementioned approximation is valid for a frequency range between $[\omega_L; \omega_H]$. The frequencies of the zeros and poles are evaluated using (22)

$$(22) \quad \omega_{z,n} = \omega_L \sqrt[n]{\rho}, \omega_{p,n} = \omega_{z,n} \sigma, \omega_{z,n+1} = \omega_{p,n} \rho$$

Such that:

$$\sigma = \left(\frac{\omega_H}{\omega_L} \right)^{\frac{\beta}{N}}, \quad \rho = \left(\frac{\omega_L}{\omega_H} \right)^{\frac{1-\beta}{N}}$$

B. Fuzzy fractional PD^μ+I controller

In Figure 5 below, an FLC is applied to the PD^μ action and the integral of the error is added to the output in order to find a fuzzy PD^μ+I controller. In this structure, the integral action cancels the final steady state error.

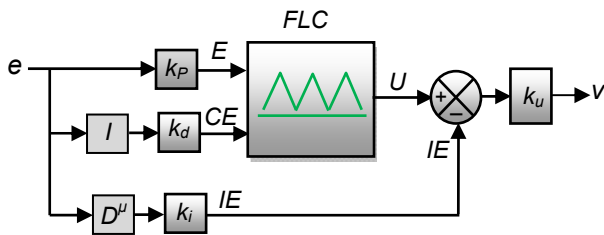


Fig.5. Fuzzy fractional PD^μ+I controller

The control action v is a nonlinear function of error E , fractional change of error CE , and integral of error IE with the following model

$$(23) \quad v(k) = [f(E, CE), IE] k_u \\ = [f(k_p e(k) + k_d D^{\mu} e(k)) + k_i Ie(k)] k_u$$

For the fuzzy PD^μ+I controller illustrated in Figure 5, the rule-base can be constructed in the following form (see Table 2):

If E is **NM** and CE is **NS** Then U is **NL**

where: NL, NM, NS, ZR, PS, PM, and PL indicate the linguistic variables "Negative Large", "Negative Medium",

"Negative Small", "Zero", "Positive Small", "Positive Medium" and "Positive Large", respectively.

Table 2. Rule base of the controller to be calibrated

E/CE	NL	NM	NS	ZR	PS	PM	PL
NL	NL	NL	NL	NL	NM	NS	ZR
NM	NL	NL	NL	NM	NS	ZR	PS
NS	NL	NL	NM	NS	ZR	PS	PM
ZR	NL	NM	NS	ZR	PS	PM	PL
PS	NM	NS	ZR	PS	PM	PL	PL
PM	NS	ZR	PS	PM	PL	PL	PL
PL	ZR	PS	PM	PL	PL	PL	PL

The membership functions for the premises and consequents of the rules are shown in Figure 6.

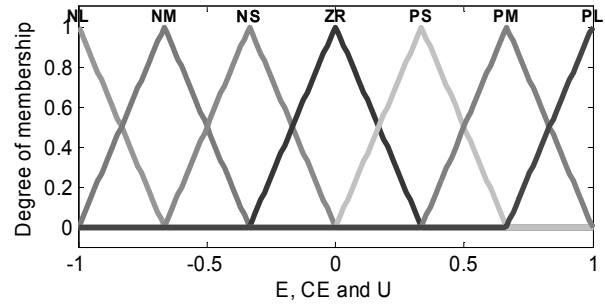


Fig.6. Membership functions for E, CE and U

The acting of all rules produces the control strategy which is presented by the nonlinear surface in Figure 7.

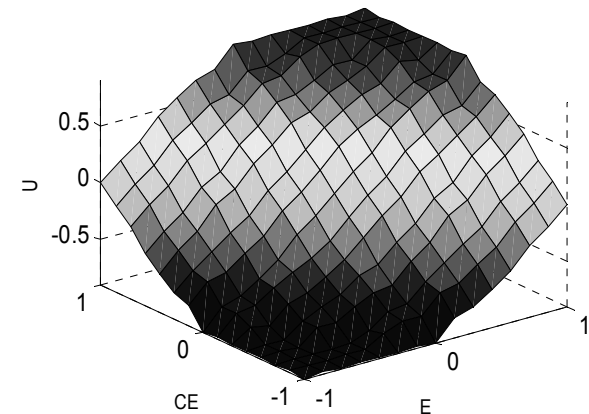


Fig.7. Control Surface

The fuzzy controller will be adjusted by changing the parameter values of k_p , k_d , k_i and k_u . The fuzzy inference mechanism operates by using the product to combine the conjunctions in the premise of the rules and in the representation of the fuzzy implication. For the defuzzification process we use the centroid method.

C Particle swarm optimization (PSO) algorithm

The particle swarm optimization (PSO) algorithm is a bio-inspired population based optimization method created by Kennedy [18-20]. This meta-heuristic algorithm is initialized with a random population of potential candidate solutions, called the 'particles'. It then explores the entire space to search for the global best-fit solution. Each particle has a position X_i and velocity V_i associated to it. The equations to update the velocity and position of a particle 'i' are given in (24) and (25), respectively.

$$(24) \quad v(t+1) = w_i v_i + c_1 r_1 (pbest_i - x_i(t)) + c_2 r_2 (gbest_i - x_i(t))$$

$$(25) \quad x_i(t+1) = x_i w(t) + v_i(t+1)$$

where: c_1, c_2 are the cognitive-coefficients, r_1, r_2 are random real-numbers and w is the inertia-weight. Updated position and velocity in PSO algorithm are illustrated in Figure 8.

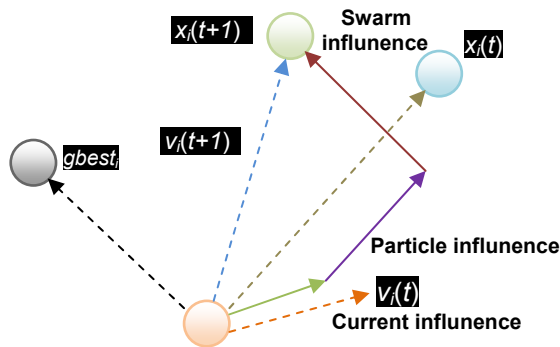


Fig.8. Position and velocity updates in PSO algorithm

D. Objective function and constraints of the present work

The integral time absolute error (ITAE) criterion is considered in this article as an objective function. The ITAE objective function is given as

$$(26) \quad ITAE = J(k_p, k_i, k_d, k_u, \mu) = \int_0^{t_{sim}} t |e(t)| dt$$

where: $e(t)$ is the error signal that is the difference between reference and actual wire-feed speeds, and t_{sim} is the simulation time, which is 2.0 s. Thereby, the problem of parameter calibration can be defined by the following optimization formulation

$$(27) \quad \begin{aligned} \text{Minimize: } J(x) \quad x &= (k_p, k_i, k_d, k_u, \mu) \in \mathfrak{R}^5 \\ &0 \leq k_p \leq 5 \\ &0 \leq k_i \leq 5 \\ \text{Subject to:} \quad &0 \leq k_d \leq 5 \\ &0 \leq k_u \leq 5 \\ &0 \leq \mu \leq 1 \end{aligned}$$

The fitness value-iteration curves from PSO tuned fuzzy PD^μ+I controller is illustrated in Figure 9. It is clear that the POS algorithm provides minimum cost function value and rapid converge.

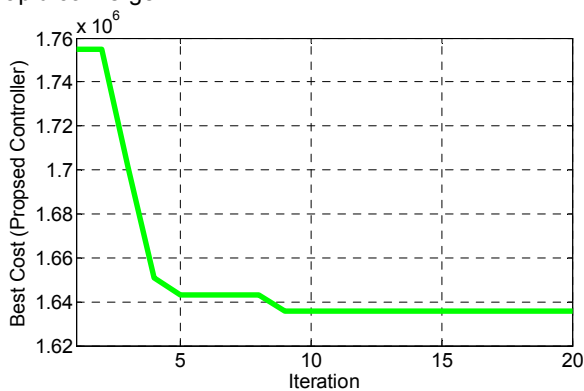


Fig.9. PSO tuned convergence plots of cost function vs iteration

The block diagram of control system employing soft computing of fuzzy fractional PD^μ+I control action is shown in Figure 10.

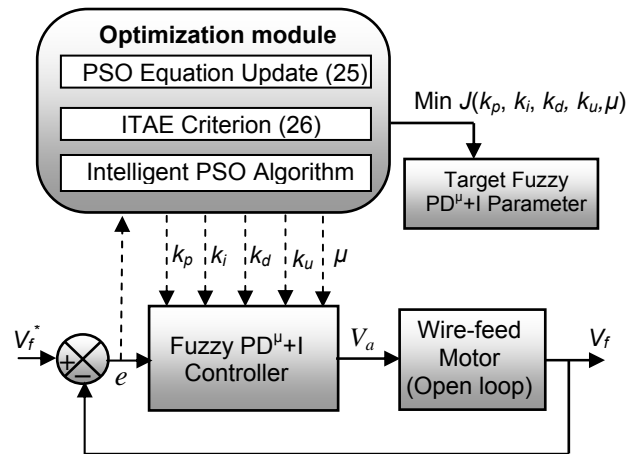


Fig.10. Proposed scheme for the parameter calibration process

Numerical simulations

In this section, four simulation tests were fulfilled based on various reference signals with external disturbances and parametric uncertainties in the PMDC motor. In each test, the efficacy of the strategies: PID, FOPID, FFOPID and the proposed fuzzy fractional PD^μ+I controller is demonstrated. In the first and second test, there are no parametric uncertainties in the PMDC motor.

For the first test the reference signal is a step curve of magnitude 1500 rpm and in the second test the reference signal is chosen as stair curves with amplitudes of 1000 rpm, 800 rpm and 1500 rpm. In the third test, a discontinuous load is implemented, i.e., the use of a torque load $T_L = 0.1$ Nm when $t \in [1, 2]$ s is considered and a torque load $T_L = 0$ Nm is utilized otherwise. In the last test, the rotary inertia J vary dynamically +20% from their nominal parameters J_0 as: $J = J_0 + 0.2 * J_0 \sin(2\pi t/3)$ when $t \in [1, 2]$ s and a $J = J_0$ is utilized otherwise.

In order to give a fair comparison between the different control algorithms, the parameter tuning for each algorithm was made by the PSO method.

Figures 11-14 illustrate the motor speed at each time instant for the best run of each control strategies for the tests: Test 1, Test 2, Test 3 and Test 4.

It is observed in Figure 11 and Figure 12 that the proposed fuzzy fractional PD^μ+I controller is the controller that more effectively regulates the speed of the PMDC motor when there are no uncertainties.

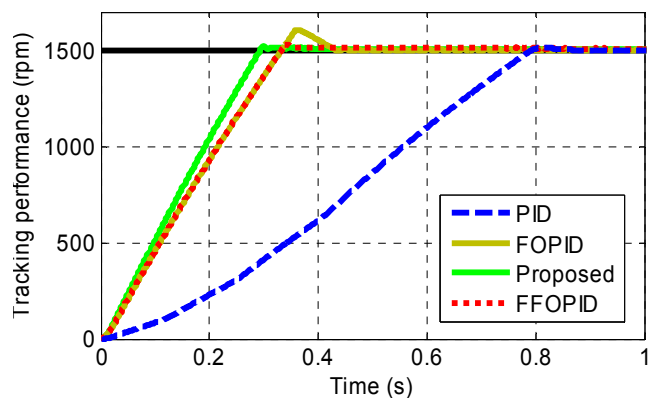


Fig.11. Control performance in Test 1

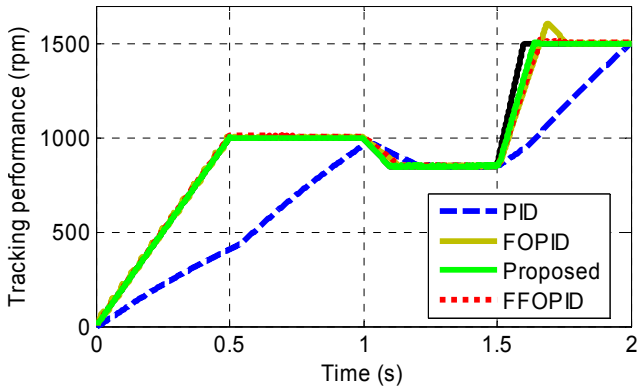


Fig.12. Control performance in Test 2

In the third test, where a discontinuous load is included into the system, Figure 13 depicts more clearly, that the proposed fuzzy fractional $PD^{\mu}+I$ controller is also the best controller. When a torque load is introduced to the PMDC motor, the speed regulation error for all controllers does not surpass $\pm 5\%$ of the desired speed with exception of the PID controller, which surpasses $+60\%$.

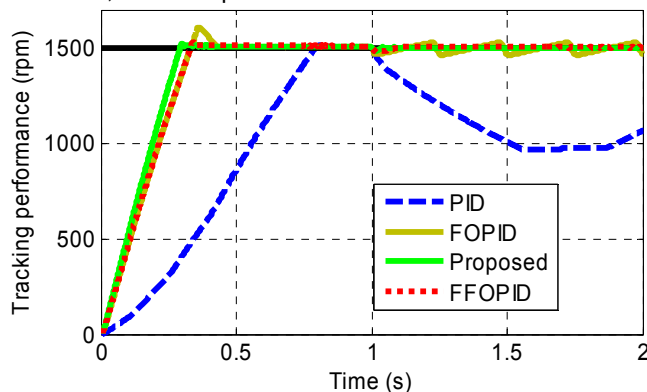


Fig.13. Control performance in Test 3

For the fourth test, where the rotary inertia is dynamical, Figure 14 illustrates that the proposed fuzzy fractional $PD^{\mu}+I$ controller is more valuable to compensate uncertainties.

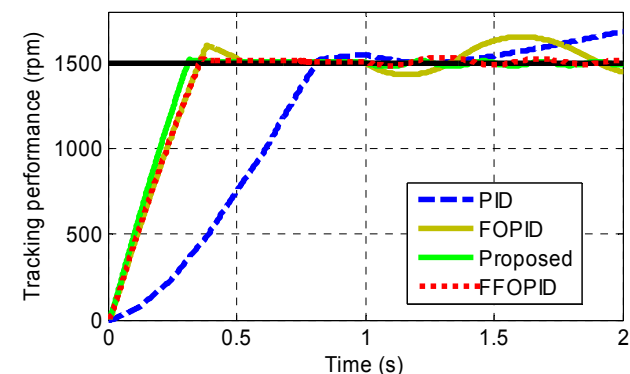


Fig.14. Control performance in Test 4

Conclusion

In this paper, a key solution to the problem of wire-feed speed regulation in GMAW process has been introduced using a robust optimal fuzzy fractional $PD^{\mu}+I$ controller. The combination of FLCs and fractional $PD^{\mu}+I$ controller yields better and robust control of wire feeder units of GMAW. Numerical simulations are carried out in Matlab/Simulink environment, and results presented and discussed. Comparison of these results with those of the PID, FOPID, and FFOPID controller is presented in each test and it is

seen that the optimized fuzzy fractional $PD^{\mu}+I$ controller is the most promising controller in the speed regulation problem of the WFUs under dynamic and discontinuous uncertainties in the PMDC motor. As a future work, the authors intend to carry out the experimental part to complete and finalize the project.

Acknowledgments

This work was supported by Reserche Center in Industrial Technologies (CRTI) and Directorate General of Scientific Research and Technological Development DGRST of Algeria.

Authors: Dr. Hamouda Noureddine, Research Center in Industrial Technologies (CRTI), P.O.Box64, Cheraga 16014 Algiers, Algeria, n.hamouda@crti.dz, Dr. Babes Badreddine, Research Center in Industrial Technologies (CRTI), P.O.Box64, Cheraga 16014 Algiers, Algeria, elect_babes@yahoo.fr, Dr. Kahla Sami, Research Center in Industrial Technologies (CRTI), P.O.Box64, Cheraga16014 Algiers, Algeria, s.kahla@crti.dz; Dr. Boutaghane Amar, Research Center in Industrial Technologies (CRTI), P.O.Box64, Cheraga16014 Algiers, Algeria, a.boutaghane@crti.dz; Dr. Hamouda Cherif, ALCIOM, 3 Rue des Vignes 78220 Viroflay, Paris, France, hamouda@alciom.com.

REFERENCES

- [1] Naidu D.S., Ozelik S., Moore K.L., Modeling sensing and control of gas metal arc welding, Elsevier publications, 2003. <https://doi.org/10.1016/B978-0-08-044066-8.X5000-9>.
- [2] Kahla S., Boutaghane A., Dehimi S., Hamouda N., Babes B., Amraoui R., Grey wolf optimization of fractional PID controller in gas metal arc welding process, In Proc. 5th International Conference on Control Engineering and Information Technology CEIT-, Sousse, Tunisia, 2017.
- [3] Greene B.W., Arc current control of a robotic welding system: modeling and control system design, B.S., University of Illinois, September 1988.
- [4] Jiluan P., Arc welding control, Woodhead Publishing Limited and CRC Press LLC © 2003, Woodhead Publishing Ltd.
- [5] Chaouch S., hasni M., Boutaghane A., Babes B., Mezaache M., Slimane S., Djenaihi M., DC-motor control using arduino board for wire-feed system, Proceedings of the IEEE, 3rd CISTEM'18 - Algiers, Algeria, October 29-31, 2018.
- [6] Hamouda N., Babes B., Hamouda C., Kahla S., Ellinger T., Petzoldt J., Optimal tuning of fractional order proportional-integral-derivative controller for wire feeder system using ant colony optimization, Journal Européen des Systèmes Automatisés, vol. 53, no. 2, pp.157-166, 2020. <https://doi.org/10.18280/jesa.530201>.
- [7] Hamouda N., Babes B., Boutaghane A., Kahla S. and Mezaache M., Optimal Tuning of $PI^{\lambda}D^{\mu}$ Controller for PMDC Motor Speed Control Using Ant Colony optimization Algorithm for Enhancing Robustness of WFSSs, 020 1st International Conference on Communications, Control Systems and Signal Processing (CCSSP), EL OUED, Algeria, 2020, pp. 364-369. doi: 10.1109/CCSSP49278.2020.9151609.
- [8] Hamouda N., Babes B., Boutaghane A., Design and analysis of robust nonlinear synergetic controller for a PMDC motor driven wire-feeder system (WFS). In Proceedings of the 4th International Conference on Electrical Engineering and Control Applications (ICEECA2019), November 19-21, 2019, Constantine, Algeria.
- [9] Paul A.K., Experimental design approach to explore suitability of PI and SMC concepts for power electronic product development, Int. J. Power Electronics, vol. 6, no. 1, pp 42-65, 2014.
- [10] Ngol M.D., Duy V.H, Phuong N.T, Kim H.K, Kim S.B., Development of digital gas metal arc welding system, Journal of Materials Processing Technology, Int. J. Power Electronics, vol. 180, no. 1, pp. 384-391, 2007.
- [11] Paul A.K., Robust PMDC motor control for accurate wire feeding in GMAW using back EMF, IEEE transactions on industrial electronics, DOI 10.1109/TIE.2019.2896131. January 2019.

- [12] Bingul Z., Karahan O., Comparison of PID and FOPID controllers tuned by PSO and ABC algorithms for unstable and integrating systems with time delay, *Optimal Contr. Appl. Methods* vol. 39, no. 4, pp. 1431-1450, 2018.
- [13] Tehrani K.A., Amirahmadi A., Rafiei S.M.R., Griva G., Barrandon L., Hamzaoui M., Rasoanarivo I., Sargos F.M., Design of fractional order PID controller for boost converter based on Multi-Objective optimization, in *Proc. 14th IEEE PEMC*, T3-179-T3-185, 2010.
- [14] Verma S.K., Yadav S., Nagar S.K., Fractional order PI controller design for non-monotonic phase systems, *IFAC-Papers OnLine*, vol. 49, no. 1, pp. 236-240, 2016.
- [15] Xu Y., Zhou J., Xue X., Fu W., Zhu W., Li C., An adaptively fast fuzzy fractional order PID control for pumped storage hydro unit using improved gravitational search algorithm, *Energ. Conver. and Manag.*, vol. 111, no. 1, pp. 67-78, 2016.
- [16] Krzysztof Oprzędkiewicz, Maciej Podsiadło, Klaudia Dziedzic., Integer order vs fractional order temperature models in the forced air heating system, *Przegląd Elektrotechniczny* 95 (2019), nr.11, 35-40
- [17] Afghoul H., Chikouche D., Krim F., Babes B., Beddar A., Implementation of fractional-order integral-plus-proportional controller to enhance the power quality of an electrical grid, *Electric Power Components and Systems*. vol. 00, no. 0, pp.1-11, 2016. DOI: 10.1080/15325008.2016.1147509.
- [18] Josip Pavleka., Srete Nikolovski., Marinko S., Finding optimal location of FACTS device for dynamic reactive power compensation using genetic algorithm and particle swarm optimisation (PSO), *Przegląd Elektrotechniczny* 95 (2019), nr.8, 86-91
- [19] Yuriy Romasevych., Viatcheslav Loveikin., Sergii Usenko., PI-controller tuning optimization via PSO-based technique, *Przegląd Elektrotechniczny* 95 (2019), nr.7, 33-37
- [20] Teja S.V., Shanavas T.N., Patnaik S.K., Modified PSO based sliding mode controller parameters for buck converter, in *Proc. 2012 IEEE, Students Conference on Electrical, Electronics and Computer Science*.